

Docking control on both stationary and moving stations based on docking formation

Ji-Wook Kwon and Jiwon Seo

A docking control algorithm of a non-holonomic mobile agent is proposed, which can be employed in both the stationary and the underway docking stations. To this end, a leader–follower docking formation is proposed, where the size of the formation is reduced until docking surfaces of the agent and the docking stations contact each other. Also, a feedback linearisation control law that can compensate for the input constraint is implemented to maintain the docking formation. Numerical simulations are included to show the performance of the proposed docking control algorithm.

Introduction: Docking control has been used in various industrial and scientific fields such as ship-to-ship mooring systems [1, 2], multiple robot systems [3], service robots [4] and aerial refuelling systems [5]. To establish the docking system, numerous control algorithms have been proposed with consideration of two types of docking stations: stationary and moving stations. Since the characteristics of the two types of docking stations are different from each other, the control algorithms have been developed separately according to the type of the docking station.

The docking control on the stationary platform should consider the approach direction of the mobile agent (i.e. this problem is similar to a posture control of a non-holonomic mobile robot [6]). On the other hand, the mobile agent can dock on the underway platform while they move side by side (i.e. this is similar to the target tracking control). However, to the authors' knowledge, a docking control algorithm, which covers both the stationary and the moving stations, has not been previously proposed in the literature.

This Letter proposes a docking control law covering both the stationary and the moving platforms based on a leader–follower (L–F) formation control algorithm [7], such that the size of the formation is reduced until the agent docks on the docking station (the station and the agent will be assigned as a leader and a follower, respectively). This docking formation is generated with respect to the docking surfaces of the station and the agent, and maintained by employing a feedback linearisation [8]. The contributions of this Letter are as follows: first, the mobile agent is able to dock in any approach direction to the stationary station with the proposed algorithm. Secondly, the mobile agent can dock in any direction of the underway station as well. Finally, these functionalities covering both the stationary and the underway stations are achieved by the same proposed docking algorithm without any algorithmic change according to the mobility of the docking station.

Trajectory generation via docking formation: Assuming that the agent is described as

$$\dot{x}_i = v_i \cos \theta_i, \quad \dot{y}_i = v_i \sin \theta_i \text{ and } \dot{\theta}_i = \omega_i \quad (1)$$

where (x, y) is a position of the agent, θ is an orientation and v and ω are the linear and angular velocities, respectively, which are designed as control inputs. The subscript, i , presents the roles of the agents; the docking station and the agent are assigned the leader, l , and the follower, f , respectively. Also, the agent has the non-holonomic constraint described by $\dot{x}_i \sin \theta_i - \dot{y}_i \cos \theta_i = 0$. From the kinematic model in (1), we propose the docking formation as depicted in Fig. 1. $L(t)$ is the distance between the leader and the desired position of the follower at a time t , which will be reduced from $L(0)$ to $(L_l + L_f)$. The desired position (x_d, y_d) is chosen as

$$x_d = x_l + L(t) \cos(\theta_l + \psi_l), \quad y_d = y_l + L(t) \sin(\theta_l + \psi_l) \quad (2)$$

Here, the angular position of the docking surface, ψ_f , of the agent is determined by the docking station as in Fig. 2. In the case of the moving platform (Fig. 2a), since the agent and the station can dock with each other while they move side-by-side or back-to-back, the angular position of the docking surface of the follower, ψ_f , is determined with respect to ψ_l as $\psi_f = \psi_l - \pi$.

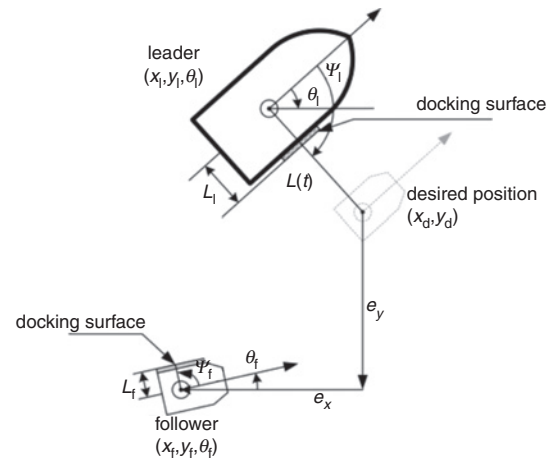


Fig. 1 Proposed docking formation with respect to docking surface

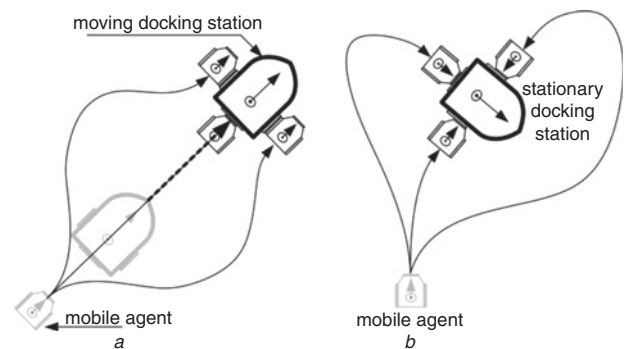


Fig. 2 Possible docking motions of agent according to mobility of docking station

- a Moving station
- b Stationary station

On the other hand, in the case of the stationary platform (Fig. 2b), since the agent has the non-holonomic constraint, the agent cannot dock on the platform side-by-side. It should dock on the platform using its docking surface in the driving direction (i.e. $\psi_f = 0$). By holding the docking formation in Fig. 1 and (2), the position errors, e_x and e_y , are expressed as

$$e_x = x_d - x_f \text{ and } e_y = y_d - y_f \quad (3)$$

whose time derivatives are

$$\begin{aligned} \dot{e}_x &= \dot{x}_l + \dot{L}(t) \cos(\theta_l + \psi_l) - L(t) \sin(\theta_l + \psi_l) \omega_l - v_f \cos \theta_f \\ \dot{e}_y &= \dot{y}_l + \dot{L}(t) \sin(\theta_l + \psi_l) + L(t) \cos(\theta_l + \psi_l) \omega_l - v_f \sin \theta_f \end{aligned} \quad (4)$$

where in the case of the stationary docking station, $\dot{x}_l, \dot{y}_l, \dot{\theta}_l = 0$.

Docking control based on feedback linearisation: To make the follower track the desired position attracted to the docking surface of the leader by $L(t)$, we employ the feedback linearisation control for the mobile agent with the non-holonomic constraint, which has been applied to trajectory tracking problems [8].

$$v_f = X_f \cos \theta_f + Y_f \sin \theta_f, \quad \omega_f = \dot{\theta}_d + k_\theta \tanh(e_\theta/k_\theta) \quad (5)$$

where $e_\theta = \theta_d - \theta_f$; $\theta_d = \text{atan2}(Y_f, X_f)$, which is a four-quadrant inverse tangent determined in the intervals $(-\pi, \pi]$ and k_θ is a positive constant. Once this control law in (5) is applied to our novel docking formulation in (2)–(4), X_f and Y_f can be expressed as follows

$$\begin{aligned} X_f &= \dot{x}_l + \dot{L}(t) \cos(\theta_l + \psi_l) - L(t) \sin(\theta_l + \psi_l) \omega_l + k_v \tanh(e_x/k_v) \\ Y_f &= \dot{y}_l + \dot{L}(t) \sin(\theta_l + \psi_l) + L(t) \cos(\theta_l + \psi_l) \omega_l + k_v \tanh(e_y/k_v) \end{aligned}$$

where k_v is a positive constant. Here, it can be noted that the control law in (5) can consider the constrained inputs because the state variables are bounded (i.e. $\dot{x}_l, \dot{y}_l, \dot{L}(t), L(t), \omega_l \in L_\infty$) and the error term is also bounded (i.e. $|k_v \tanh(\cdot)| \leq k_v$). If it is assumed that there is an autopilot

system of the mobile agent realising the motion control inputs in (5) based on the kinematics, the proposed control inputs are applicable with stability to the actual systems such as the system in Fig. 1 (refer to [8] to ensure the feasibility of this assumption and the control law in (5)).

Simulation results: For numerical simulations, we employ two scenarios as follows. In the scenarios, the leader has three docking surfaces $\psi_l = \{-\pi/2, \pi/2, \pi\}$, $L_l = 0.5$ m and $L(t) = -\tanh((t - \alpha)/\beta) + \gamma$, where $\alpha = 5$ m, $\beta = 5$ m and $\gamma = 2$ m. Also, for the follower, $L_f = 0.5$ m.

In the first scenario, the follower docks on the stationary station. The leader position is $(x_l, y_l, \theta_l) = (3, 3, -\pi/3)$ and the initial position of the follower is $(x_f, y_f, \theta_f) = (2, 0, \pi/2)$. The routes of the follower docking on the three docking surfaces of the leader are depicted in Fig. 3.

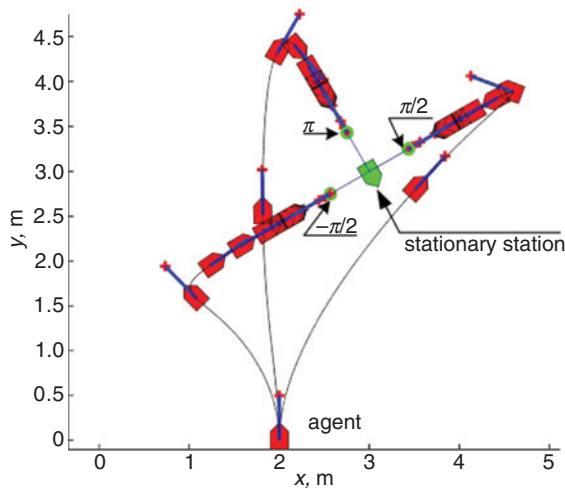


Fig. 3 Routes of follower docking on three docking surfaces of stationary leader (+: docking surface of follower and \circ : docking surfaces of leader)

As can be seen in Fig. 3, the follower with the proposed docking control algorithm moves towards the docking surfaces of the leader while following the approach direction. To show the performance of the docking algorithm on the stationary platform, Fig. 4 shows the distance errors of the three cases of $\psi_f = \{-\pi/2, \pi/2, \pi\}$. In Fig. 4, the distance errors converge to zero as time advances.

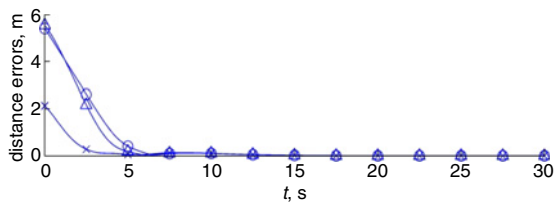


Fig. 4 Distance errors of follower docking on three docking surfaces of stationary leader (+: $\psi_f = -\pi/2$, Δ : $\psi_f = \pi/2$, \circ : $\psi_f = \pi$)

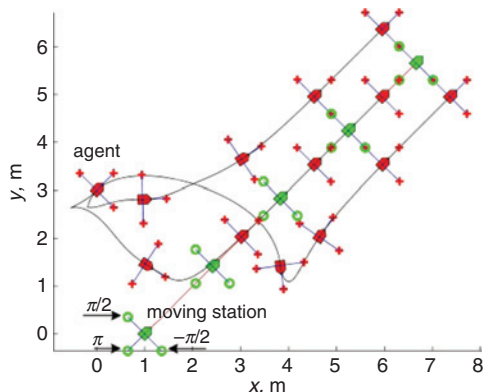


Fig. 5 Routes of follower docking on three docking surfaces of underway leader (+: docking surfaces of follower, \circ : docking surfaces of leader)

The second scenario shows that the follower docks on the three docking surfaces of the moving leader. The initial condition of the leader is $(x_l(0), y_l(0), \theta_l(0)) = (1, 0, \pi/4)$, the linear and the angular velocities are $v_l = 0.4$ m/s and $\omega_l = 0$ rad/s, respectively and the initial condition of the follower is $(x_f(0), y_f(0), \theta_f(0)) = (0, 3, \pi/4)$. The routes of the follower docking on the three docking surfaces of the leader are depicted in Fig. 5.

Fig. 5 shows that it is possible that the follower docks on any sides of the underway leader while moving side-by-side or back-to-back with the leader. To show the performance of the docking algorithm on the moving platform, Fig. 6 shows the distance errors of the three cases. The distance errors converge to zero as time advances.

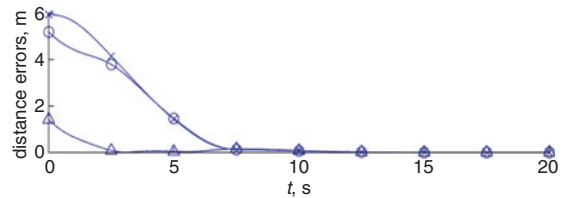


Fig. 6 Distance errors of followers docking on three docking surfaces of underway leader (+: $\psi_f = -\pi/2$, Δ : $\psi_f = \pi/2$, \circ : $\psi_f = \pi$)

Conclusion: We propose a docking control algorithm covering the stationary and the underway docking stations based on our docking formation where the size of the formation is reduced until a docking surface of the agent contacts a docking surface of the station. It is ensured that the mobile agent with the non-holonomic constraint docks on any surface of the docking station using the same algorithm regardless of the mobility of the station.

Acknowledgment: This research was supported by the MSIP (Ministry of Science, ICT and Future Planning), Korea, under the 'IT Consilience Creative Program' (NIPA-2014-H0201-14-1001) supervised by the NIPA (National IT Industry Promotion Agency).

© The Institution of Engineering and Technology 2014

7 February 2014

doi: 10.1049/el.2014.0467

One or more of the Figures in this Letter are available in colour online.

Ji-Wook Kwon (Yonsei Institute of Convergence Technology, Yonsei University, Songdogwahak-ro, Yeonsu-gu, Incheon 406-840, Republic of Korea)

Jiwon Seo (School of Integrated Technology, Yonsei University, Songdogwahak-ro, Yeonsu-gu, Incheon 406-840, Republic of Korea)

E-mail: jiwon.seo@yonsei.ac.kr

References

- Kim, Y.Y., Choi, K.-J., Chung, H., and Lee, P.-S.: 'Axiomatic design study for automatic ship-to-ship mooring system for container operations in open sea'. *Ocean Syst. Eng.*, 2011, **1**, (2), pp. 157–169
- Breivik, M., and Loberg, J.-E.: 'A virtual target-based underway docking procedure for unmanned surface vehicles'. IFAC World Congress, Milan, Italy, August 2011, pp. 13630–13635
- Seo, J., Yim, M., and Kumar, V.: 'Assembly planning for planar structure of a brick wall pattern with rectangular modular robots'. IEEE Proc. Int. Conf. Automation Science and Engineering, Madison, WI, USA, August 2013, pp. 1016–1021
- Muse, D., Weber, C., and Wermter, S.: 'Robot docking based on omnidirectional vision and reinforcement learning'. *Knowledge-Based Syst.*, 2006, **19**, (5), pp. 324–332
- Cetin, O., and Yilmaz, G.: 'Sigmoid limiting functions and potential field based autonomous air refueling path planning for UAVs'. *J. Intell. Robot. Syst.*, 2014, **73**, (1–4), pp. 797–810
- Chwa, D., Hong, S.-K., and Song, B.: 'Robust posture stabilization of wheeled mobile robots in polar coordinates'. Proc. Int. Symp. Mathematical Theory of Networks and Systems, Kyoto, Japan, July 2006, pp. 343–348
- Kwon, J.-W., and Chwa, D.: 'Hierarchical formation control based on a vector field method for wheeled mobile robots'. *IEEE Trans. Robot.*, 2012, **28**, (6), pp. 1335–1345
- Chwa, D.: 'Tracking control of differential-drive wheeled mobile robots using a backstepping-like feedback linearization'. *IEEE Trans. Syst. Man Cybern., Part A*, 2010, **40**, (6), pp. 1285–1295